

# HEAVE ADDED MASS AND DAMPING OF A PERFORATED DISK BELOW THE FREE SURFACE

B. MOLIN\*, F.G. NIELSEN\*\*

\* Ecole Supérieure d'Ingénieurs de Marseille, 13451 Marseille cedex 20, molin@esim.fr

\*\* Norsk Hydro ASA, P.O. Box 7190, N-5020 Bergen, finn.gunnar.nielsen@hydro.com



Figure 1: Experimental protection cover.

The photograph above shows a 1:21 model of a protection cover, used to shelter bottom equipment used in offshore oil production, such as well-heads. The full scale dimensions are about 20 m  $\times$  15 m. As can be seen in the picture it consists in a tubular frame with an open area ratio around 35 %. Other designs have lower porosity ratios (15-20 %).

An operational problem is the installation of such structures, from the surface crane ship down to the sea-floor. One must check that the loads exerted on the structure itself and on the hoist are within tolerable limits. Therefore it is desirable to evaluate the hydrodynamic properties of such structures. For standard "large bodies" this is done classically through linearized potential flow theory: hydrodynamic coefficients are expressed as added mass and damping matrices, frequency dependent (due to the free surface) but amplitude independent, and wave excitation loads. Viscous effects are sometimes introduced *a posteriori* via a drag term, giving an amplitude-dependent correction to the damping.

Decay or forced motion tests in still water of models such as shown in figure 1 have revealed that not only the damping but also the added mass depend, to a large extent, on the motion amplitude.

In 1990 Molin & Legras proposed a theoretical model to derive the added mass and damping of a truncated vertical cylinder with slots: it consisted in replacing the alternance of solid and open parts by a uniform porosity, applying a **quadratic** relationship between the pressure differential and traversing velocity, and recurring to the usual linearized potential flow theory. This provided amplitude-dependent hydrodynamic coefficients in good agreement with values derived from model tests. Since then the same approach has been applied to a variety of problems and geometries like vertical or horizontal plates (Molin & Fourest, 1992; Molin, 2001a), shrouded cylinders (Molin, 1993) and periodic arrays of perforated disks in unbounded fluid domain (Molin, 2001b). The latter case being relevant to the stabilizing plates incorporated to the truss spars.

In this paper we consider the closely related case of one single perforated disk in-between the free surface and sea-floor. The disk undergoes forced vertical motion in the absence of waves. The motion amplitude is assumed to be small so that boundary conditions can be set at the mean positions of the disk and free surface. The only non-linearity introduced in the problem is the "discharge equation" that relates the pressure drop and relative fluid velocity through the porous disk.

The fluid domain is bounded by the bottom ( $z = 0$ ) and the free surface ( $z = h$ ). The disk radius is  $a$  and it is located at a distance  $d$  from the bottom. The fluid is divided into 3 sub-domains: an outer domain 1 ( $R \geq a$ ,  $0 \leq z \leq h$ ), a domain 2 below the disk ( $R \leq a$ ,  $0 \leq z \leq d$ ), and a domain 3 above the disk ( $R \leq a$ ,  $d \leq z \leq h$ ).

We take  $W = A\omega \cos\omega t$  as the imposed vertical velocity and we use potential flow theory. For a solid disk this is an acceptable assumption as long as the Keulegan-Carpenter number is sufficiently small. For a perforated disk we must also make sure that the flow separates through the openings and that the rotational wakes remain confined within a short distance of the disk. This means that the openings must be small (and numerous enough to be idealized as uniform porosity). Then it makes some sense to use potential flow theory to describe the outer flow.

As in Molin (2001b) the discharge equation is taken under the form

$$p_2 - p_3 = \rho \frac{1 - \tau}{2\mu\tau^2} (\Phi_z - A\omega \cos\omega t) |\Phi_z - A\omega \cos\omega t|. \quad (1)$$

Here  $\tau$  is the porosity ratio (open area divided by total area) and  $\mu$  a discharge coefficient (usually in-between 0.5 and 1).

Equation (1) is partly linearized into

$$\varphi_2 - \varphi_3 = -\frac{i}{\omega} \frac{8}{3\pi} \frac{1 - \tau}{2\mu\tau^2} (\varphi_z - A\omega) \|\varphi_z - A\omega\| \quad (2)$$

where  $\|\cdot\|$  stands for the modulus of the complex number and  $\Phi(R, z, t) = \Re\{\varphi(R, z) \exp(-i\omega t)\}$ .

The boundary value problem to be solved is then:

$$\Delta\varphi = 0 \quad \text{in the fluid} \quad (3)$$

$$g\varphi_z - \omega^2\varphi = 0 \quad \text{at the mean free surface } z = h \quad (4)$$

$$\varphi_2 - \varphi_3 = -\frac{i}{\omega} \frac{8}{3\pi} \frac{1 - \tau}{2\mu\tau^2} (\varphi_z - A\omega) \|\varphi_z - A\omega\| \quad \text{on the disk } z = d \quad 0 \leq R \leq a \quad (5)$$

$$\varphi_z = 0 \quad \text{on the bottom } z = 0 \quad (6)$$

$$\text{radiation condition} \quad R \rightarrow \infty \quad (7)$$

At the outer edge of the disk the pressure differential is nil. Hence the traversing velocity is also zero. We take advantage of this feature to expand  $\varphi_z(R, d)$  as

$$\varphi_z(R, d) = A\omega \left[ 1 + \sum_{i=1}^{\infty} D_i J_0(\nu_i R) \right] \quad (8)$$

where the "wave numbers"  $\nu_i$  are the roots of  $J_0(\nu_i a) = 0$ . This provides an orthogonal basis over the disk.

The BVP is solved through eigen-function expansions, with the velocity potential being developed as:

- Sub-domain 1

$$\varphi_1(R, z) = A\omega a \left\{ A_0 \frac{\cosh k_0 z}{\cosh k_0 h} \frac{H_0(k_0 R)}{H_0(k_0 a)} + \sum_{n=1}^{N_1} A_n \cos k_n z \frac{K_0(k_n R)}{K_0(k_n a)} \right\} \quad (9)$$

- Sub-domain 2

$$\varphi_2(R, z) = \frac{A\omega}{2d} \left( z^2 - \frac{R^2}{2} \right) + A\omega a \left\{ B_0 + \sum_{n=1}^{N_2} B_n \cos \lambda_n z \frac{I_0(\lambda_n R)}{I_0(\lambda_n a)} \right\} + A\omega \sum_{i=1}^{N_4} \frac{D_i}{\nu_i} \frac{\cosh \nu_i z}{\sinh \nu_i d} J_0(\nu_i R) \quad (10)$$

- Sub-domain 3

$$\begin{aligned} \varphi_3(R, z) = & A\omega \left[ z - h + \frac{g}{\omega^2} \right] + A\omega a \left\{ C_0 \frac{\cosh \mu_0(z - d)}{\cosh \mu_0(h - d)} J_0(\mu_0 R) + \sum_{n=1}^{N_3} C_n \cos \mu_n(z - d) \frac{I_0(\mu_n R)}{I_0(\mu_n a)} \right\} \\ & + A\omega \sum_{i=1}^{N_4} \frac{D_i}{\nu_i} \left( \delta_i \cosh \nu_i(z - d) + \sinh \nu_i(z - d) \right) J_0(\nu_i R) \end{aligned} \quad (11)$$

where

$$\omega^2 = g k_0 \tanh k_0 h = -g k_n \tan k_n h = g \mu_0 \tanh \mu_0 (h - d) = -g \mu_n \tan \mu_n (h - d) \quad (12)$$

$$\delta_i = \frac{\omega^2 \tanh \nu_i (h - d) - g \nu_i}{g \nu_i \tanh \nu_i (h - d) - \omega^2} \quad (13)$$

and  $J_0, I_0, K_0, H_0 = J_0 + iY_0$  are the standard notations for Bessel and Hankel functions.

The conditions that remain to be fulfilled are the matching equations for  $\varphi$  and  $\varphi_R$  at  $R = a$ , and the discharge equation. The difficulty arising from its non-linearity is overcome through an iterative procedure whereby equation (5) is written as

$$\sum_j \left[ -\frac{8i}{3\pi} \widetilde{K}_C f(R) - \frac{\coth \nu_j d - \delta_j}{\nu_j a} \right] D_j J_0(\nu_j R) = \frac{1}{2ad} \left( d^2 - \frac{R^2}{2} \right) - \frac{1}{a} \left( d - h + \frac{g}{\omega^2} \right) + B_0 + \sum_n (-1)^n B_n \frac{I_0(\lambda_n R)}{I_0(\lambda_n a)} - C_0 \frac{J_0(\mu_0 R)}{\cosh \mu_0 (h - d)} - \sum_n C_n \frac{I_0(\mu_n R)}{I_0(\mu_n a)} \quad (14)$$

where  $\widetilde{K}_C$  is the "porous Keulegan-Carpenter number", defined as (cf Molin, 2001b):

$$\widetilde{K}_C = \frac{1 - \tau}{2\mu\tau^2} \frac{A}{a} \quad (15)$$

and  $f(R) = \|\sum_i D_i J_0(\nu_i R)\|$  is evaluated from the solutions obtained at the previous iterations.

Multiplying both sides of equation (14) with  $R J_0(\nu_i R)$  and integrating in  $R$  from 0 to  $a$  for  $i = 1, \dots, N_4$  gives the linear system

$$\mathbf{M}^{(i)} \cdot \vec{D}^{(i)} = \vec{E}_D + \mathbf{DB} \cdot \vec{B}^{(i)} + \mathbf{DC} \cdot \vec{C}^{(i)} \quad (16)$$

Similarly the matching conditions at  $R = a$  result into the vectorial equations (applying a procedure *à la* Garrett, 1971):

$$\vec{B}^{(i)} = \vec{E}_{21} + \mathbf{BA} \cdot \vec{A}^{(i)} \quad (17)$$

$$\vec{C}^{(i)} = \vec{E}_{31} + \mathbf{CA} \cdot \vec{A}^{(i)} \quad (18)$$

$$\vec{A}^{(i)} = \vec{E}_1 + \mathbf{AB} \cdot \vec{B}^{(i)} + \mathbf{AC} \cdot \vec{C}^{(i)} + \mathbf{AD} \cdot \vec{D}^{(i)} \quad (19)$$

Eliminating  $\vec{A}^{(i)}, \vec{B}^{(i)}$  and  $\vec{C}^{(i)}$  in-between equations (16) through (19) gives a linear system in  $\vec{D}^{(i)}$  which is solved by a standard Gauss routine. Convergence is reached within a few iterations. The complex added mass coefficient is then obtained by

$$\frac{M_{33}}{\rho a^3} = C_a + i C_b = 2\pi \left[ \frac{2h - d}{4a} - \frac{a}{16d} - \frac{g}{2a\omega^2} + \frac{B_0}{2} + \sum_{n=1}^{N_2} (-1)^n \frac{\beta_n B_n}{\lambda_n a} - \frac{J_1(\mu_0 a) C_0}{\mu_0 a \cosh \mu_0 (h - d)} - \sum_{n=1}^{N_3} \frac{\gamma_n C_n}{\mu_n a} + \sum_{i=1}^{N_4} (\coth \nu_i d - \delta_i) \frac{D_i}{\nu_i^2 a^2} J_1(\nu_i a) \right] \quad (20)$$

where  $\beta_n = I_1(\lambda_n a)/I_0(\lambda_n a)$  and  $\gamma_n = I_1(\mu_n a)/I_0(\mu_n a)$ .

## Comparison with experimental results

Tests were performed at Marintek with different hatch models, but, unfortunately, always in mid-water, away from the free surface and bottom, in quasi infinite fluid conditions.

The model shown in figure 1 was submitted to forced motion tests. Added mass and damping were derived from the force record. In the calculations the rectangular frame was idealized by a disk of same area. Figure 2 shows the experimental hydrodynamic coefficients vs. the calculated ones, with a porosity ratio of 35 % and a  $\mu$  coefficient of 0.75. They are given vs. the "porous Keulegan-Carpenter number"  $\widetilde{K}_C$  (equation 15).

Figure 3 shows results obtained with two other models of smaller size, with a length over width ratio of 2 (not quite circular) and open area ratios of 16 and 25 %. The added mass and damping coefficients were derived from decay tests. Again the calculations were done for a disk of identical area. It should be noted that the calculated results in figure 3 are just the same as in figure 2: in infinite fluid the non-dimensional added mass and damping coefficients only depend on  $\widetilde{K}_C$ . This time the agreement is good for the added mass coefficient but strong

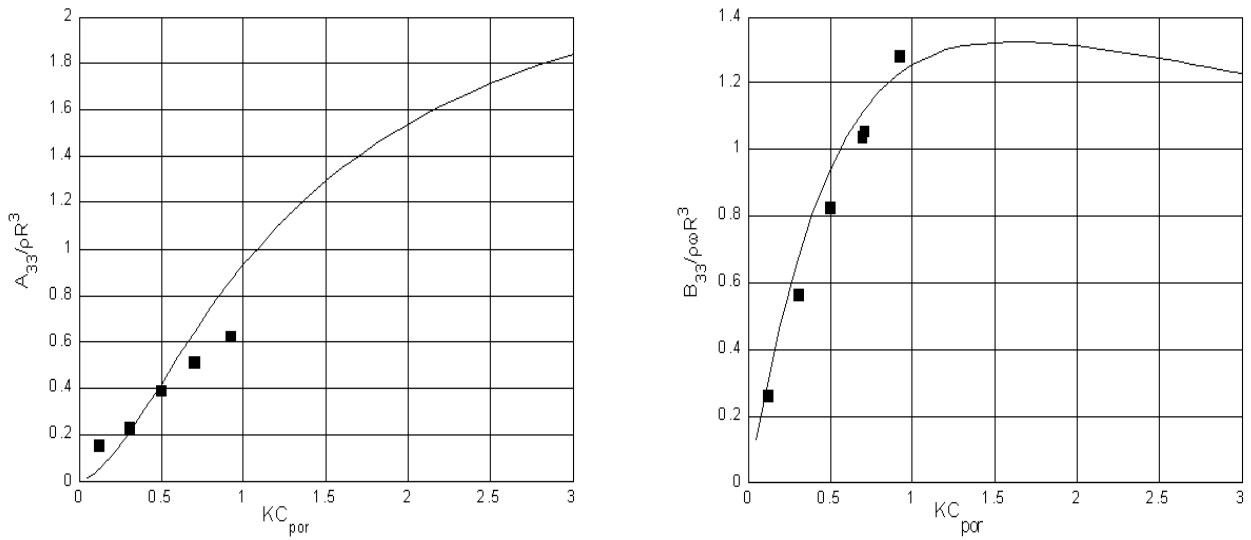


Figure 2: Added mass and damping coefficients from forced motion tests. Calculated (lines) vs. measured values.

deviations occur for the damping when  $\widetilde{K}_C$  becomes larger than 1. This is presumably due to vortex shedding from the outer edge which is not taken into account by the present theory and which becomes dominant when  $\widetilde{K}_C \rightarrow \infty$ .

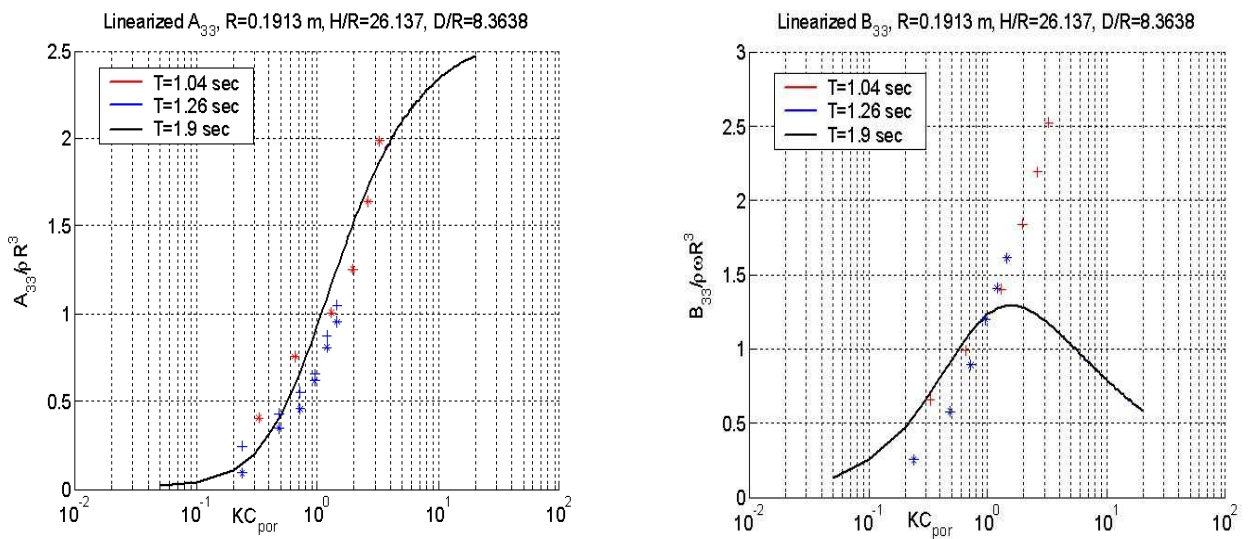


Figure 3: Added mass and damping coefficients from decay tests. Calculated (lines) vs. measured values.

## References

- GARRETT C.J.R. 1971 Wave forces on a circular dock, *J. Fluid Mech.*, **46**, 129-139.
- MOLIN B. 1993 A potential flow model for the drag of shrouded cylinders. *J. Fluids & Structures*, **7**, 29-38.
- MOLIN B. 2001a Numerical and physical wave-tanks. Making them fit, *Ship Technology Research*, **48**, 2-22.
- MOLIN B. 2001b On the added mass and damping of periodic arrays of fully or partially porous disks, *J. Fluids & Structures*, **15**, 275-290.
- MOLIN B. & LEGRAS J-L. 1990 Hydrodynamic modeling of the Roseau tower stabilizer. In *Proc. 9th Int. Conf. Offshore Mechanics & Arctic Engineering (OMAE)*, Vol I, Part B, 329-336.
- MOLIN B. & FOUREST J-M. 1992 Numerical modeling of progressive wave absorbers. In *Proc. 7th Int. Workshop Water Waves & Floating Bodies*, 199-203.

**Discussor:** R. Porter

Presumably there is a singularity in the fluid velocity at the edge of the disk. The matching conditions you use (matching pressure and horizontal velocity across  $r = a$ ) take no account of this singularity. Does this result in a slowly convergent system of equations for your unknown coefficients?

**Author's reply:**

For sure the strong singularity has an effect on the convergence of the series. As an illustration, here are the added mass and damping coefficients obtained in the case  $h = 10\text{m}$ ,  $d = 9\text{ m}$ ,  $a = 10\text{ m}$  and  $T = 10\text{ sec}$ , as functions of the truncation order  $N$  (with  $N_1 = N_2 = N_3 = N$ , the disk being solid).

$N$	$C_a$	$C_b$
10	11.56044	18.68005
20	11.30441	19.18106
50	11.14161	19.46748
100	11.09415	19.55812
200	11.06849	19.60234
400	11.05578	19.62413

**Discussor:** Q.W. Ma

Good agreement has been shown between experimental and calculated results for the cases with a horizontal disk in vertical motions. I would like to know if you have results about the influence of the angle of the disk with respect to the horizontal direction. I am also grateful if you would make comments on how to modify equation (1) to deal with the case where a disk is not horizontal.

**Author's reply:**

If the disk is not horizontal equation (1) will still hold with the relative velocity taken in the normal direction. The resolution will have to be fully numerical with the disk represented by appropriate singularities.